

Published in final edited form as:

*Eur J Radiol.* 2013 May ; 82(5): 734–739. doi:10.1016/j.ejrad.2011.09.021.

## Musculoskeletal MRI at 3.0T and 7.0T: A Comparison of Relaxation Times and Image Contrast

Caroline D. Jordan<sup>1,2</sup>, Manojkumar Saranathan<sup>1</sup>, Neal K. Bangerter<sup>3</sup>, Brian A. Hargreaves<sup>1</sup>, and Garry E. Gold<sup>1</sup>

Caroline D. Jordan: cjordan@stanford.edu; Manojkumar Saranathan: manojsar@stanford.edu; Neal K. Bangerter: nealb@ee.byu.edu; Brian A. Hargreaves: bah@stanford.edu; Garry E. Gold: gold@stanford.edu

<sup>1</sup>Department of Radiology at Stanford

<sup>2</sup>Department of Bioengineering at Stanford

<sup>3</sup>Department of Electrical & Computer Engineering, Brigham Young University, Provo, UT

### Abstract

**OBJECTIVE**—The purpose of this study was to measure and compare the relaxation times of musculoskeletal tissues at 3.0T and 7.0T, and to use these measurements to select appropriate parameters for musculoskeletal protocols at 7.0T.

**MATERIALS AND METHODS**—We measured the  $T_1$  and  $T_2$  relaxation times of cartilage, muscle, synovial fluid, bone marrow and subcutaneous fat at both 3.0T and 7.0T in the knees of five healthy volunteers. The  $T_1$  relaxation times were measured using a spin-echo inversion recovery sequence with six inversion times. The  $T_2$  relaxation times were measured using a spin-echo sequence with seven echo times. The accuracy of both the  $T_1$  and  $T_2$  measurement techniques was verified in phantoms at both magnetic field strengths. We used the measured relaxation times to help design 7.0T musculoskeletal protocols that preserve the favorable contrast characteristics of our 3.0T protocols, while achieving significantly higher resolution at higher SNR efficiency.

**RESULTS**—The  $T_1$  relaxation times in all tissues at 7.0T were consistently higher than those measured at 3.0T, while the  $T_2$  relaxation times at 7.0T were consistently lower than those measured at 3.0T. The measured relaxation times were used to help develop high resolution 7.0T protocols that had similar fluid-to-cartilage contrast to that of the standard clinical 3.0T protocols for the following sequences: proton-density-weighted fast spin-echo (FSE),  $T_2$ -weighted FSE, and 3D-FSE-Cube.

**CONCLUSION**—The  $T_1$  and  $T_2$  changes were within the expected ranges. Parameters for musculoskeletal protocols at 7.0T can be optimized based on these values, yielding improved resolution in musculoskeletal imaging with similar contrast to that of standard 3.0T clinical protocols.

---

© 2011 Elsevier Ireland Ltd. All rights reserved.

**Authors Contact Info:** <sup>1</sup>Address: The Richard M. Lucas Center for Imaging, Mail Code 5488, Stanford, CA 94305-5488, Phone: (650) 723-5945, Fax: 650-723-5795

<sup>3</sup>Address: 469 CB, Brigham Young University, Provo, Utah 84602, Phone: 801-422-4869

**Publisher's Disclaimer:** This is a PDF file of an unedited manuscript that has been accepted for publication. As a service to our customers we are providing this early version of the manuscript. The manuscript will undergo copyediting, typesetting, and review of the resulting proof before it is published in its final citable form. Please note that during the production process errors may be discovered which could affect the content, and all legal disclaimers that apply to the journal pertain.

## Keywords

MR Relaxometry; musculoskeletal; 7.0T; relaxation times

---

## Introduction

Magnetic resonance imaging (MRI) at higher magnetic field strengths offers several advantages over imaging at lower magnetic field strengths. Signal-to-noise ratio (SNR) is expected to increase with increasing magnetic field strength due to the increased spin polarization. The increased SNR can often be traded for higher spatial resolution or decreased scan time<sup>1-3</sup>. Certain cartilage imaging techniques, such as *in vivo* sodium imaging, may be improved at 7.0T since *in vivo* sodium imaging has the challenges of lower SNR, limited spatial resolution, and long acquisition times<sup>3</sup>. Tissue contrast is dependent on the repetition time (TR) and the echo time (TE) of the sequence. Knowledge of the T<sub>1</sub> and T<sub>2</sub> relaxation times of musculoskeletal tissues at 7.0T is important for obtaining image contrast similar to that of existing methods at lower magnetic field strengths. Relaxation times are also important to know for their biochemical significance.

However, there are also distinct disadvantages to scanning at higher magnetic field strengths. Currently, 7.0T MRI is not FDA-approved for clinical use. Additional disadvantages include increased specific absorption ratio (SAR) effects from the increased radiofrequency (RF) power deposition, greater B<sub>0</sub> and B<sub>1</sub> magnetic field inhomogeneities, and increased chemical shift artifacts from fat<sup>2, 3</sup>.

Previous studies of <sup>1</sup>H NMR relaxation times indicate that T<sub>1</sub> is expected to increase with increasing field strength according to a general curve of the form  $T_1 = A\nu^B$ , where  $\nu$  is the Larmor frequency, and A and B are constants that have been fit for the specific tissue<sup>4</sup>.

For example, this previous work calculated  $A = 0.000455$  and  $B = 0.4203$  for skeletal tissue, and at 7.0T,  $\nu$  is about 298 MHz. Although these studies indicate that the observed T<sub>2</sub> is independent of magnetic field strength, more recent work in musculoskeletal tissues has found that T<sub>2</sub> typically decreases with increasing magnetic field strength<sup>4-7</sup>. Thus in our experiment, we expect T<sub>1</sub> to increase substantially and T<sub>2</sub> to decrease slightly at 7.0T compared to the relaxation times at 3.0T<sup>5, 7</sup>.

There have been a number of studies measuring T<sub>1</sub> and T<sub>2</sub> relaxation times in musculoskeletal tissues at different magnetic field strengths. Several studies have previously measured and compared musculoskeletal relaxation measurements at 1.5T, 3.0T and 4.0T. One representative study found an average T<sub>1</sub> increase from 1.5T to 3.0T of about 20%, and a slight average T<sub>2</sub> decrease<sup>5</sup>. Another study found that T<sub>1</sub> values increased for all tissues from 1.5 T to 4.0T, while T<sub>2</sub> values decreased by 10–20% for all tissues except for bone marrow<sup>6</sup>. Several studies of cartilage tissue at 3.0T and 7.0T found that cartilage T<sub>1</sub> values increased by about 35%, while cartilage T<sub>2</sub> values decreased or remained about the same<sup>7, 8</sup>. Knowledge of relaxation times is necessary to develop musculoskeletal protocols at 7.0T.

This study differs from previous work in that we measured and compared the T<sub>1</sub> and T<sub>2</sub> relaxation times of five human musculoskeletal tissues in the knee at both 3.0T and 7.0T in a single subject population, and then used these measurements to select appropriate parameters for musculoskeletal MRI methods at 7.0T that provide similar fluid-to-cartilage contrast to that of current 3.0T clinical protocols.

## Materials and Methods

A total of twelve healthy volunteers were enrolled in this study (4 females, 8 males, ages 22–39, mean age 28.7). For the  $T_1$  measurements, the right knees of a set of five healthy volunteers were imaged on a 3.0T GE Discovery whole body scanner, and on a 7.0T GE Magnex whole body scanner for the  $T_1$  measurements (GE Healthcare, Waukesha, WI, USA). Since one volunteer who was scanned at 7.0T was not able to be scanned at 3.0T, a sixth volunteer was scanned as a replacement at 3.0T only. The right knees of another set of five healthy volunteers were imaged at both 3.0T and 7.0T for the  $T_2$  measurements. All scans were done under a protocol approved by the local institutional review board. A Nova Medical quadrature birdcage transmit-receive knee coil was used at 7.0T for the volunteers and the phantoms (Nova Medical, Wilmington, MA, USA). At 3.0T, a GE eight-channel receive/quadrature transmit knee coil was used to scan volunteers, and a single-channel quadrature birdcage Invivo coil was used to scan a volunteer for the clinical standard 3.0T protocols and the peanut oil phantoms (Invivo, Gainesville, FL, USA).

### $T_1$ Relaxation Time Measurement Protocol

The  $T_1$  relaxation times were measured using a spin-echo inversion recovery (SE-IR) sequence with six different inversion times (TI) spaced logarithmically (approximately) along a hypothetical  $T_1$  recovery curve. The  $T_1$  relaxation times were calculated by performing a fit of the mean pixel signal intensities of a selected region of interest (ROI) at the different inversion times. The inversion pulse was an adiabatic Silver-Hoult pulse, with a pulse width of 8640  $\mu$ s at both 3.0T and 7.0T. Table 1 shows the inversion times, and the sequence parameters for 3.0T and 7.0T. Taking into consideration the effects of incomplete  $T_1$  recovery due to the 8000ms repetition time, we used a nonlinear least squares regression fit to find  $M_0$ ,  $T_1$ , and  $\epsilon$  in MATLAB using the following equation,

$$M_i = M_0 e^{-TE/T_2} \{1 - (2+\epsilon) e^{-TI/T_1} + (1+\epsilon) e^{-(TR-TE/2)/T_1} - (1+\epsilon) e^{-TR/T_1}\}, \quad (1)$$

where the small  $\epsilon$  term accounts for an imperfect inversion pulse (MathWorks, Natick, MA, USA)<sup>9</sup>.  $M_0$  and  $e^{-TE/T_2}$  are both independent of TI, and so we combined their fit in the calculation. We then calculated the regression coefficient  $R^2$  to determine the goodness of fit.

### $T_2$ Relaxation Time Measurement Protocol

The  $T_2$  relaxation times were measured using a spin-echo (SE) sequence by calculating an exponential fit of the mean pixel signal intensities of a selected ROI at seven echo times. Table 1 shows the logarithmically spaced echo times and the scan sequence parameters for both 3.0T and 7.0T. Again taking into consideration the effects of incomplete  $T_1$  recovery due to the 4500ms repetition time, we used a nonlinear least squares regression fit to find  $M_0$  and  $T_2$  in MATLAB, using the following equation,

$$M_i = M_0 e^{-TE/T_2} \{1 - 2e^{-(TR-TE/2)/T_1} + e^{-TR/T_1}\}, \quad (2)$$

where  $T_1$  is the averaged measured  $T_1$  value from the previous measurements<sup>9</sup>. The regression coefficient,  $R^2$ , was calculated for each fit to determine the goodness of fit.

We used only the last five echo time points to fit the synovial fluid curve, since the echo time spacing of these points was more appropriate for the expected longer  $T_2$  value. We used only the first five echo time points for the other four tissues with expected shorter  $T_2$  values, as the last two echo time points had very low SNR for these tissues. To maintain the

accuracy of the relaxation curve  $t_1$ , points below or near the noise floor or with extremely low SNR were discarded to avoid biasing the fit.

For both sets of measurements, relaxation times were averaged across all subjects and the standard deviations of the measurements were calculated. The statistical significance of differences between the 3.0T and 7.0T measurements was calculated using a paired Student's  $t$ -test, and the  $p$ -values were recorded.

### Phantom Validation

$T_1$  and  $T_2$  measurements were performed twice on different days for reproducibility on a vial of peanut oil at both 3.0T and 7.0T. These measurements were used to assess repeatability of the fitting methods. We used the same  $T_1$  and  $T_2$  fitting protocols for fat as described above and calculated the regression coefficient  $R^2$  for each fit.

### Data Processing

For each scan, a single axial slice with a 16cm field-of-view (FOV) and slice thickness of 3mm was acquired through a region in the knee that included five musculoskeletal tissue types: patellar cartilage, lateral gastrocnemius muscle, femoral bone marrow, patellofemoral joint fluid, and medial subcutaneous fat. A region of interest (ROI) was drawn within each tissue type, and the mean signal intensity was recorded for each signal curve fitting. ROIs in the synovial fluid and cartilage were relatively small because of the smaller volumes of tissue present. The ROI of the patellar cartilage was chosen such that it was directly posterior to the cortical bone of the patella.

### 7.0T Protocol Design

Based on the measured  $T_1$  and  $T_2$  relaxation times, the fluid-to-cartilage image contrast ratio was estimated for the following 3.0T clinical sequences: proton-density (PD) weighted fast spin-echo (FSE),  $T_2$ -weighted FSE, and 3D-FSE-Cube with isotropic resolution<sup>10-12</sup>. Figure 1A shows how we found the pixel with the closest signal to the simulated fluid-cartilage contrast ratio at 3.0T, and then chose the corresponding TE and TR for each sequence at 7.0T. We imaged the left knee of a healthy 29-year-old male volunteer at 3.0T, using the standard clinical protocols, and at 7.0T, using our optimized 7.0T protocols on different days. The measured fluid-to-cartilage contrast ratio was estimated by calculating the SNR in a region of interest in each tissue, and taking the ratio of the mean SNRs. The flip angle train of the 3D-FSE-Cube was optimized at 7.0T for minimizing the SAR.

## Results

### Phantom results

Table 2 lists the measured  $T_1$  and  $T_2$  relaxation times of peanut oil at both 3.0T and 7.0T from the repeated scans of the peanut oil phantom, the percent change in relaxation times between the repeated scans, the percent increase or decrease in relaxation times between magnetic field strengths and the average regression coefficient  $R^2$ . The phantom measurements demonstrate that the  $T_1$  and  $T_2$  measurement method is repeatable over time, as the percent changes between the repeated scans are small. We measured a 55% increase in the  $T_1$  of peanut oil from 3.0T to 7.0T, similar to our measured average increase in  $T_1$  of 51% for musculoskeletal tissues *in vivo* (described below). We measured a 24% decrease in the  $T_2$  of peanut oil from 3.0T to 7.0T, similar to our measured average decrease in  $T_2$  of 21% for musculoskeletal tissues *in vivo* (also described below).

## In vivo results

Table 3 shows the measured  $T_1$  relaxation times at 3.0T and 7.0T, the percent increase, and the p-value, demonstrating a statistically significant increase from 3.0T to 7.0T for all tissues. The regression coefficient  $R^2$  is greater than or equal to 0.99 for all fits. The average increase in  $T_1$  relaxation times was 51%. Table 4 shows the measured  $T_2$  relaxation times at both 3.0T and 7.0T, the percent decrease, and the p-value demonstrating significant decrease for all tissues. The regression coefficient  $R^2$  is greater than or equal to 0.99 for all fits. The average decrease in  $T_2$  relaxation times was 21%.

### 7.0T protocol design results

The relaxation times were used to develop examples of very high-resolution 7.0T protocols for a PD-weighted FSE sequence, a T<sub>2</sub>-weighted FSE sequence, and a 3D-FSE-Cube sequence. The 7.0T sequence parameters were chosen to mimic as closely as possible the fluid-to-cartilage contrast obtained by the standard clinical protocols at 3.0T, while achieving significantly higher resolution. Figure 1 demonstrates the importance of choosing the appropriate TE and TR at different magnetic field strengths. Figure 1B and 1C demonstrate the theoretical signals from musculoskeletal tissues as a function of TR for a spin-echo sequence at 3.0T and 7.0T using the measured  $T_1$  and  $T_2$  values, given a TE of 15ms.

Figure 2 shows the images from the three sequences used in our standard clinical protocol at 3.0T and the three sequences comprising our example protocol at 7.0T. The 7.0T protocol achieves a significant increase in the in-plane image resolution relative to the 3.0T protocol for each of the sequences while yielding similar image contrast. Table 5 shows the scan parameters for all three sequences.

Figure 2A shows PD-weighted FSE images with an in-plane resolution of 0.29mm × 0.47mm at 3.0T, while in Figure 2B, the 7.0T sequence achieves an in-plane resolution of 0.15mm × 0.20 mm (a 4.8x reduction in voxel volume at 7.0T). The measured fluid-to-cartilage contrast ratios for the PD-weighted FSE images were 1.9 and 2.4 at 3.0T and 7.0T respectively.

Figure 2C shows T<sub>2</sub>-weighted FSE images at 3.0T with an in-plane resolution of 0.39mm × 0.47mm, while in Figure 2D, the 7.0T sequence achieves an in-plane resolution of 0.20mm × 0.29mm (a 3.2x reduction in voxel volume at 7.0T vs. 3.0T). The measured fluid-to-cartilage contrast ratios for the T<sub>2</sub> FSE sequence were 4.2 and 3.9 at 3.0T and 7.0T respectively.

Figure 2E shows 3D-FSE-Cube images at 3.0T with an in-plane resolution of 0.50mm × 0.59mm, while in Figure 2F, the 7.0T sequence achieves an in-plane resolution of 0.39mm × 0.59mm (a 1.3x reduction in voxel volume at 7.0T). The measured fluid-to-cartilage contrast ratios for the 3D-FSE-Cube sequence were 4.2 and 2.6 at 3.0T and 7.0T respectively.

Figure 3 demonstrates higher SNR efficiency at 7.0T than at 3.0T for all tissues for the three sequences. The SNR measurements at 7.0T are scaled relative to the in-plane voxel size and the square root of total readout time.

## Discussion

Our  $T_1$  measurements at 3.0T are in reasonable agreement with values reported in the literature. Our cartilage  $T_1$  measurements at 3.0T and 7.0T are close to literature values, although may be slightly lower due to the ROI chosen in the deeper region of the patellar cartilage<sup>8, 13</sup>. Our muscle and synovial fluid  $T_1$  measurements at 7.0T were lower than the

$T_1$ s measured at 4.0T. This could be due to different measurement biases in our spin-echo inversion-recovery sequence relative to the Look-Locker sequence<sup>6</sup>. The lower repetition time used to keep scan times reasonable may affect the  $T_1$  and  $T_2$  measurements for synovial fluid, due to incomplete signal recovery. Our synovial fluid  $T_1$  measurements at 3.0T are also lower than a similar study's measurements at 3.0T, again perhaps due to our use of the spin-echo inversion-recovery sequence, instead of a Look-Locker sequence<sup>5</sup>. A previous study found the 3D fast Look Locker sequence obtained accurate  $T_1$  relaxation times, although they noted that it did tend to slightly over-estimate  $T_1$  values<sup>14</sup>. A detailed study of the measurement bias of each of these techniques is needed, but is beyond the scope of the present study.

Our  $T_2$  measurements are also in good agreement with values reported in the literature. Our cartilage  $T_2$  measurements at 7.0T were consistent with a previous study's measurement of cartilage in the deep cartilage layer<sup>7</sup>. Our fat and bone marrow  $T_2$  values at 3.0T are lower than those of a previous study, perhaps due to our use of a spin-echo sequence instead of a spiral  $T_2$  preparation sequence<sup>5</sup>. The choice of  $T_1$  was important to finding accurate nonlinear  $T_2$  fits for synovial fluid, so we used the average measured  $T_1$  value from this study.

A 256×128 matrix size was used for the  $T_1$  and  $T_2$  measurements to keep scan times reasonable; however, this limited the number of pixels in the ROIs. The reduced resolution may lend itself to partial-volume effects from the surrounding tissue and may reduce the  $T_1$  value, particularly in small ROIs, such as the ROIs for cartilage and fluid. For the  $T_1$  measurements, only six inversion times were used, ranging from 50ms to 3600ms, so that exam time would be kept reasonable. A longer inversion time might have been helpful for the synovial fluid  $T_1$  fit.

We designed three 7.0T musculoskeletal protocols based on fast spin-echo sequences. However, the signal equation we used to theoretically estimate the fluid-to-cartilage image contrast was based on the spin-echo signal equation (2). The choice of parameters for the FSE images at 7.0T might improve the sequence and its contrast if a fast spin-echo algorithm is used. A recent study has optimized clinical ankle sequences and demonstrated higher SNR and contrast-to-noise ratio (CNR) at 7.0T over 3.0T, using a QED 28 channel dedicated knee coil at 7.0T (QED, Mayfield Village, OH, USA)<sup>15</sup>.

The primary goal of developing these musculoskeletal methods at 7.0T was to obtain ultra high spatial resolution images, and a similar fluid-to-cartilage contrast to that of the standard clinical protocols at 3.0T. Further studies are needed to do a more detailed comparison between the achievable SNR and SNR efficiency of the optimized protocols at 7.0T vs. 3.0T.

## Conclusion

In summary, we measured the  $T_1$  and  $T_2$  relaxation times in five musculoskeletal tissues at both 3.0T and 7.0T in a single subject population, and verified our methods in phantoms. For all five tissues at 7.0T, the  $T_1$  relaxation times increased by an average of 51%, whereas the  $T_2$  relaxation times decreased by an average of 21%. We used these measurements to help optimize parameters for several musculoskeletal sequences at 7.0T that achieved both high spatial resolution and similar fluid-to-cartilage image contrast as that of standard 3.0T clinical protocols. Knowledge of these relaxation parameters will enable further parameter optimization for musculoskeletal imaging protocols at 7.0T.

## Acknowledgments

We would like to thank Kyunghyun Sung, Joshua Kaggie, and Ernesto Staroswiecki for discussions regarding non-linear fitting. This project was supported by the Richard M. Lucas Foundation, the NCCR Center of Advanced MR Technology at Stanford P41RR09784, NIH EB002524, the Arthritis Foundation, and GE Healthcare.

## References

1. Collins CM, Smith MB. Signal-to-noise ratio and absorbed power as functions of main magnetic field strength, and definition of “90 degrees ” RF pulse for the head in the birdcage coil. *Magn Reson Med*. 2001; 45(4):684–91. [PubMed: 11283997]
2. Vaughan JT, Snyder CJ, DelaBarre LJ, et al. Whole-body imaging at 7T: preliminary results. *Magn Reson Med*. 2009; 61(1):244–8. [PubMed: 19097214]
3. Regatte RR, Schweitzer ME. Ultra-high-field MRI of the musculoskeletal system at 7.0T. *J Magn Reson Imaging*. 2007; 25(2):262–9. [PubMed: 17260399]
4. Bottomley PA, Foster TH, Argersinger RE, Pfeifer LM. A review of normal tissue hydrogen NMR relaxation times and relaxation mechanisms from 1–100 MHz: dependence on tissue type, NMR frequency, temperature, species, excision, and age. *Med Phys*. 1984; 11(4):425–48. [PubMed: 6482839]
5. Gold GE, Han E, Stainsby J, et al. Musculoskeletal MRI at 3.0 T: relaxation times and image contrast. *AJR Am J Roentgenol*. 2004; 183(2):343–51. [PubMed: 15269023]
6. Duwell SH, Ceckler TL, Ong K, et al. Musculoskeletal MR imaging at 4 T and at 1.5 T: comparison of relaxation times and image contrast. *Radiology*. 1995; 196(2):551–5. [PubMed: 7617876]
7. Welsch GH, Apprich S, Zbyn S, et al. Biochemical (T2, T2\* and magnetisation transfer ratio) MRI of knee cartilage: feasibility at ultra-high field (7T) compared with high field (3T) strength. *Eur Radiol*. 2011; 21(6):1136–43. [PubMed: 21153551]
8. Pakin SK, Cavalcanti C, La Rocca R, Schweitzer ME, Regatte RR. Ultra-high-field MRI of knee joint at 7.0T: preliminary experience. *Acad Radiol*. 2006; 13(9):1135–42. [PubMed: 16935725]
9. Bernstein, MA.; King, KF.; Zhou, XJ. *Handbook of MRI pulse sequences*. Burlington, MA: Elsevier Academic Press; 2004.
10. Gold GE, Busse RF, Beehler C, et al. Isotropic MRI of the knee with 3D fast spin-echo extended echo-train acquisition (XETA): initial experience. *AJR Am J Roentgenol*. 2007; 188(5):1287–93. [PubMed: 17449772]
11. Bauer JS, Banerjee S, Henning TD, et al. Fast high-spatial-resolution MRI of the ankle with parallel imaging using GRAPPA at 3 T. *AJR Am J Roentgenol*. 2007; 189(1):240–5. [PubMed: 17579177]
12. Mugler JP 3rd, Bao S, Mulkern RV, et al. Optimized single-slab three-dimensional spin-echo MR imaging of the brain. *Radiology*. 2000; 216(3):891–9. [PubMed: 10966728]
13. Watanabe A, Boesch C, Obata T, Anderson SE. Effect of multislice acquisition on T1 and T2 measurements of articular cartilage at 3T. *J Magn Reson Imaging*. 2007; 26(1):109–17. [PubMed: 17659569]
14. Henderson E, McKinnon G, Lee TY, Rutt BK. A fast 3D look-locker method for volumetric T1 mapping. *Magn Reson Imaging*. 1999; 17(8):1163–71. [PubMed: 10499678]
15. Juras V, Welsch G, Bar P, et al. Comparison of 3T and 7T MRI clinical sequences for ankle imaging. *Eur J Radiol*. 2011

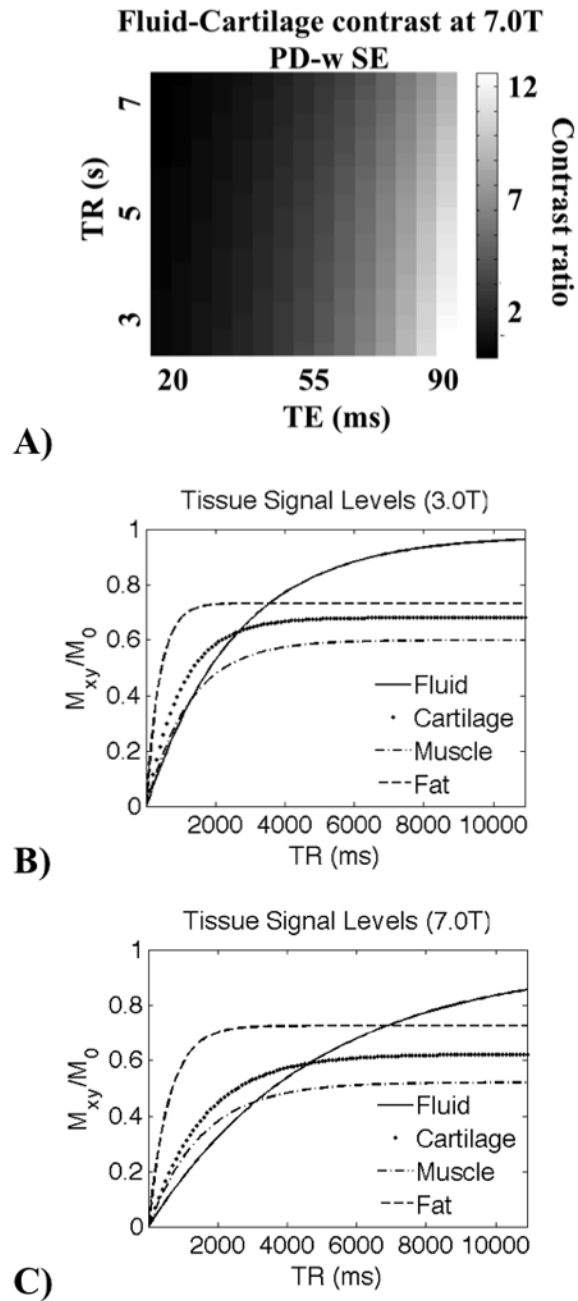


**Figure 1.**

This figure demonstrates the approximate difference in signal levels at varying relaxation times, and the importance of choosing appropriate TEs and TRs at different magnetic field strengths. In **A)** we show simulated fluid-to-cartilage contrast at 7.0T for a PD-weighted SE sequence as a function of TE and TR. This graph was used to match the calculated contrast at 3.0T. Theoretical tissue signal levels for a spin-echo sequence (equation 2) at 3.0T **B)** and 7.0T **C)** are plotted at a fixed TE (15ms), over a range of repetition times using the measured relaxation times.



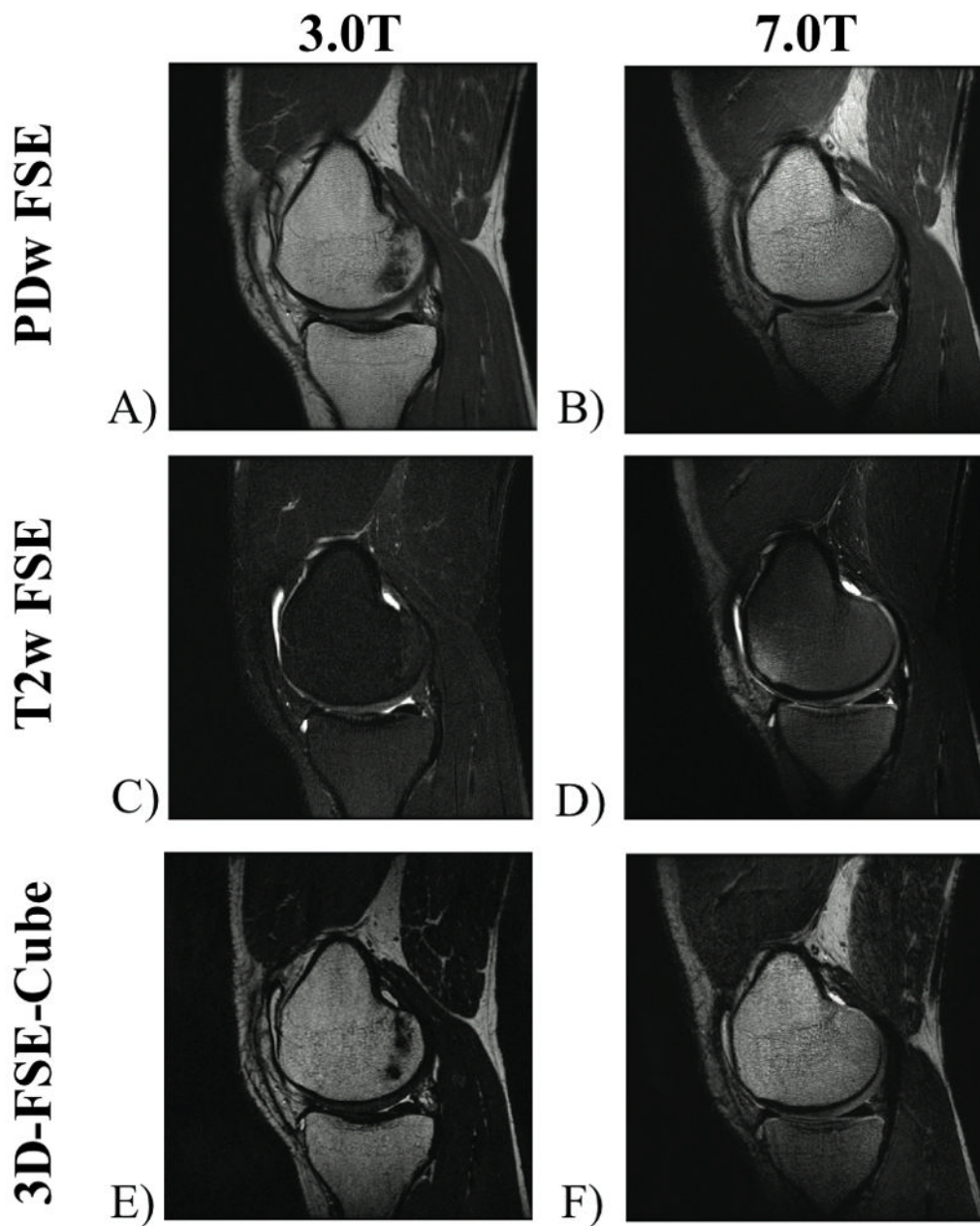


**Figure 2.** Sagittal knee protocol images acquired at 3.0T and 7.0T. The 7.0T images have higher resolution, while maintaining similar fluid-to-cartilage contrast at each magnetic field strength with in-plane resolution of **A)**  $0.29\text{mm} \times 0.47\text{mm}$ , **B)**  $0.15\text{mm} \times 0.20\text{mm}$ , (a 4.8x reduction in voxel volume at 7.0T). **C)**  $0.39\text{mm} \times 0.47\text{mm}$ , **D)**  $0.20\text{mm} \times 0.29\text{mm}$ , (a 3.2x reduction in voxel volume at 7.0T). **E)**  $0.50\text{mm} \times 0.59\text{mm}$ , **F)**  $0.39\text{mm} \times 0.59\text{mm}$ , (a 1.3x reduction in voxel volume at 7.0T).

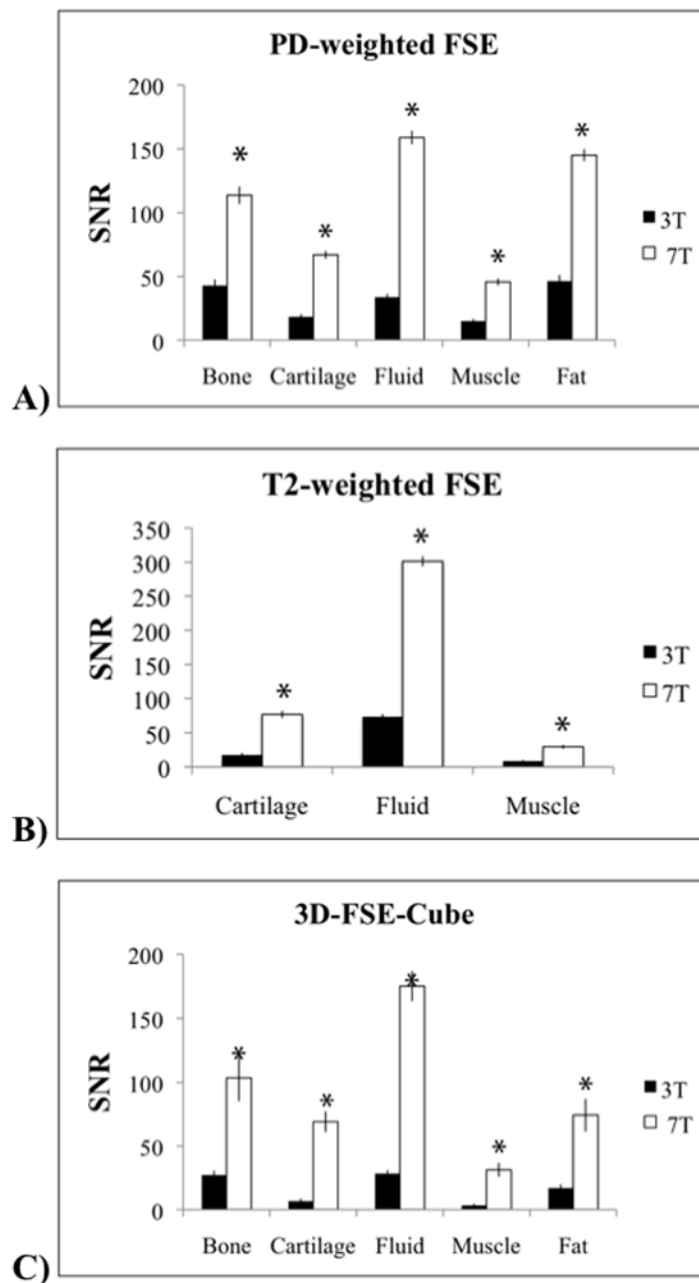


**Figure 3.** SNR efficiency is higher at 7.0T for all tissues for the three protocols. SNR measurements at 7.0T are scaled by the relative voxel size and the square root of total readout time. The asterisks indicate significantly higher SNR efficiency for the following sequences: **A)** proton density-weighted fast spin-echo (FSE) **B)** T2-weighted FSE and **C)** 3D-FSE-Cube.

**Table 1**

Spin-echo inversion recovery and spin-echo protocols at both 3.0T and 7.0T

| Parameter  | SE-IR                           | SE                              |
|------------|---------------------------------|---------------------------------|
| Matrix     | 256×128                         | 256×128                         |
| TR (ms)    | 8000                            | 4500                            |
| TE (ms)    | 15                              | [10, 20, 40, 80, 160, 320, 640] |
| TI         | [50, 150, 450, 900, 1800, 3600] | N/A                             |
| BW (kHz)   | 31.25                           | 62.5                            |
| FOV (cm)   | 16                              | 16                              |
| Scan Plane | Axial                           | Axial                           |
| NEX        | 0.75                            | 1                               |

**Table 2**

Repeated peanut-oil phantom measurements of  $T_1$  and  $T_2$  relaxation times at 3.0T and 7.0T

|            | 3.0T Scan 1 | 3.0T Scan 2 | % change between scans | 7.0T Scan 1 | 7.0T Scan 2 | % change between scans | % change between 3.0T and 7.0T | Average $R^2$ |
|------------|-------------|-------------|------------------------|-------------|-------------|------------------------|--------------------------------|---------------|
| $T_1$ (ms) | 281         | 280         | 0.3%                   | 433         | 435         | 0.5%                   | 55% increase                   | 0.99          |
| $T_2$ (ms) | 53.9        | 58.8        | 8.3%                   | 43.4        | 42.7        | 1.6%                   | 24% decrease                   | 0.99          |

**Table 3***In vivo*T<sub>1</sub> Relaxation times at 3.0T and 7.0T

| Tissue                       | T <sub>1</sub> (ms) at 3.0T | T <sub>1</sub> (ms) at 7.0T | % Increase | p-value |
|------------------------------|-----------------------------|-----------------------------|------------|---------|
| Patellar Cartilage           | 1015.6 ± 71.1               | 1568.1 ± 335.0              | 54.4       | 0.028   |
| Subcutaneous Fat             | 403.8 ± 17.7                | 583.1 ± 22.1                | 44.4       | 2.4e-5  |
| Femoral Bone Marrow          | 381.2 ± 8.0                 | 548.7 ± 11.8                | 43.9       | 1.4e-5  |
| Lateral Gastrocnemius Muscle | 1255.9 ± 57.9               | 1552.5 ± 97.3               | 23.6       | 0.007   |
| Synovial Fluid               | 2564.7 ± 269.7              | 4813.2 ± 701.4              | 87.7       | 0.007   |

**Table 4***In vivo*T<sub>2</sub> relaxation times at 3.0T and 7.0T

| Tissue                       | T <sub>2</sub> (ms) at 3.0T | T <sub>2</sub> (ms) at 7.0T | % Decrease | p-value |
|------------------------------|-----------------------------|-----------------------------|------------|---------|
| Cartilage                    | 39.1 ± 1.3                  | 31.7 ± 3.4                  | 18.9       | 0.020   |
| Subcutaneous Fat             | 48.3 ± 0.8                  | 46.1 ± 1.7                  | 4.5        | 0.019   |
| Femoral Bone Marrow          | 51.5 ± 1.2                  | 46.7 ± 0.8                  | 9.1        | 0.001   |
| Lateral Gastrocnemius Muscle | 29.3 ± 1.1                  | 23.0 ± 1.0                  | 21.6       | 0.003   |
| Synovial Fluid               | 652.9 ± 113.4               | 324.5 ± 60.9                | 50.2       | 0.016   |

**Table 5**

Sequence parameters of the clinical 3.0T and designed 7.0T protocols

| Parameter           | PD-FSE          |                 | T2-FSE          |                 | 3D-FSE-Cube     |                 |
|---------------------|-----------------|-----------------|-----------------|-----------------|-----------------|-----------------|
|                     | 3.0T            | 7.0T            | 3.0T            | 7.0T            | 3.0T            | 7.0T            |
| TE                  | 29ms            | 24ms            | 80ms            | 74ms            | 81ms            | 84ms            |
| TR                  | 3000ms          | 4500ms          | 4200ms          | 5000ms          | 2800ms          | 3000ms          |
| BW                  | 31.25kHz        | 31.25kHz        | 31.25kHz        | 31.25kHz        | 50kHz           | 50kHz           |
| Matrix              | 512×320         | 1024×768        | 384×320         | 768×512         | 288×256×124     | 384×256×124     |
| Slices              | 21              | 21              | 15              | 15              | -               | -               |
| FOV                 | 15cm            | 15cm            | 15cm            | 15cm            | 15cm            | 15cm            |
| Slice Thickness     | 2.5mm           | 2.5mm           | 2.5mm           | 2.5mm           | 0.6mm           | 0.6mm           |
| Spacing             | 0.5mm           | 0.5mm           | 0.5mm           | 0.5mm           | -               | -               |
| NEX                 | 1               | 1               | 2               | 2               | 0.5             | 0.75            |
| Freq. Dir.          | S/I             | S/I             | S/I             | S/I             | S/I             | S/I             |
| Flip Angle          | 90              | 90              | 90              | 90              | 90              | 90              |
| ETL                 | 6               | 6               | 8               | 8               | 80              | 80              |
| In-plane resolution | 0.29mm x 0.47mm | 0.15mm x 0.20mm | 0.39mm x 0.47mm | 0.20mm x 0.29mm | 0.50mm x 0.59mm | 0.39mm x 0.59mm |
| Scan time           | 2:48            | 9:40            | 5:40            | 10:45           | 8:28            | 6:45            |